Journal of the Brazilian Society of Mechanical Sciences and Engineering (2024) 46:528
https://doi.org/10.1007/s40430-024-05086-4

TECHNICAL PAPER

Design and analysis of rehabilitation hand based on segmented multi-chamber actuator

Huadong Zheng[1] · Wei Bai[1] · Caidong Wang[1] · Xinjie Wang[1] · Linxiao Liu[1]

Received: 19 July 2023 / Accepted: 13 July 2024 / Published online: 2 August 2024

Abstract
The soft rehabilitation hand has become a research hotspot in the field of robotics due to its good environmental adaptability and coupling safety. To make the soft rehabilitation hand have a large degree of freedom and strong driving force, as well as being comfortable and lightweight to wear, this paper designs a segmented multi-chamber actuator soft rehabilitation glove based on the principle of bionics. The actuators of different finger types and bone segments, which are also various in shape and size, are assembled in parallel to realize diverse movement forms of fingers. The motion deformation mechanism of the rehabilitation hand is studied, and the driving effect of the soft finger is analyzed with the help of ABAQUS finite element analysis software. 3D printing technology and pouring molding technology were used to make segmented soft rehabilitation finger physical prototype. The accuracy of the simulation model was verified by comparison and analysis of simulation data and experimental data. Simultaneously driving three brake joints through a rehabilitation single finger from 0 to 60 kPa, the motion trajectory and bending angles were tracked. A comparative analysis between simulation data and experimental data was conducted to validate the accuracy of the simulation model.

Keywords Soft robot · Segmented actuators · Rehabilitation glove · Finite element simulation

1 Introduction

In recent years, evolving bionics and materials science have brought a whole new research direction to robotics. Traditional rigid robots are characterized by fast output speed, sufficient power, high accuracy, and mature technology [1, 2], but they cannot pass through channels with dimensions smaller than their own or with complex shapes. Complex structures, poor adaptability, and expensive sensing materials make rigid robots more suitable for applications in structured environments [3]. Compared with rigid robots, soft robots have good flexibility, human–machine interaction, and relative safety, which makes bionic soft robots have excellent application prospects in key areas with high requirements for flexibility and safety of human–machine-environment interaction, such as medical surgery, assisted rehabilitation, fragile body sorting, non-structural environment detection, and underwater operation [4–6].

Among the flexible rehabilitation gloves, it contains use cord-driven rehabilitation gloves; smart materials and polymer-driven rehabilitation gloves; pneumatic-driven rehabilitation gloves, etc. [7]. Among them, cord-driven rehabilitation gloves still mainly consist of rigid structures, while materials such as polymers are less effective in the control part compared to pneumatic rehabilitation gloves. The rehabilitation glove, designed by the University of Toronto in 2020 [8], mimics a tendon-driven approach that uses a battery-driven linear motor to drive the flexion and extension of the finger. The device integrates the drive system and control system in one, and the glove opens in a

Technical Editor: Rogério Sales Gonçalves.

✉ Caidong Wang
vwangcaidong@163.com

Huadong Zheng
hurd_cheng@163.com

Wei Bai
15639741663@163.com

Xinjie Wang
wangxinjie@zzuli.edu.cn

Linxiao Liu
liulinxiao2023@163.com

[1] School of Mechanical and Electrical Engineering, Zhengzhou University of Light Industry, Zhengzhou 450002, China

folded manner for easy donning, with the disadvantage of being heavy and not conducive to finger movement. The exoskeletal rehabilitation glove, designed by Chen Jian of South-east University [9], has a silicone rubber airbag as the actuator to achieve flexion and inversion movements and a TPU nylon composite fabric airbag as the actuator to achieve extension movements, which takes up a little area in the uninflated state and is therefore mounted on the inside of the glove and secured with velcro and straps. This rehabilitation exoskeleton device is highly adaptable and can help patients to perform a variety of rehabilitation exercises with more freedom of movement and better joint flexibility. The exoskeleton glove designed by the Tokyo Institute of Technology in Japan in 2020 can assist people to play the piano better [10]. Each of its fingers is driven by four pneumatic artificial muscles to mimic the muscles and tendons in the physiological structure of the fingers. It not only controls finger movements but also enables more precise and rapid finger movements by adjusting the stiffness of each joint of each exoskeleton. In addition, the device can be driven at high frequencies, up to 10 Hz for a single finger. The incorporation of a braking system is a pivotal stage in the design of soft rehabilitation hands, particularly within the realm of rehabilitation hand design. The utilization of internally soft devices (ISDs), driven by fluid pressure, is employed for crafting actuators in soft robotic systems. These actuators encompass internal fluid channels, expanding and inducing motion in response to heightened fluid pressure [11]. The McKibben pneumatic artificial muscle (PAM) has been judiciously chosen as the braking system. This choice empowers the soft robotic glove to furnish effective hand rehabilitation support for stroke patients [12].

The existing soft body rehabilitation hand is expensive, complex in structure, not flexible enough, and has little driving force, which limits the application in hand rehabilitation training. To address the above problems, this paper designs a new soft bionic wearable rehabilitation hand with a segmented pneumatic grid structure, and conducts the analysis of the deformation mechanism, simulation, and experimental study of single finger bending motion for the designed soft rehabilitation hand.

2 Bionic mechanism of rehabilitation gloves

To achieve better finger rehabilitation training, the design of the soft rehabilitation hand structure must conform to the human finger structure and movement rules. The human hand is composed of multiple bones connected by joints and has multiple degrees of freedom [13]. The human hand skeleton is shown in Fig. 1 [14]. The four fingers, except the thumb, consist of the proximal phalanx (PP), the middle phalanx (MP), the distal phalanx (DP) and the distal interphalangeal joint (DIP), the proximal interphalangeal joint (PIP), and the metacarpophalangeal joint (MCP). The thumb consists of the proximal phalanx (PP), the distal phalanx (DP), the interphalangeal joint (IP), the metacarpophalangeal joint (MCP), and the carpometacarpal joint (CMC). The metacarpophalangeal joint of the human hand has two degrees of freedom, allowing for bend/stretch and adduction/abduction movements in the horizontal plane, where bend and stretch movements refer to the fist clenching and extension movements of the human hand. Abduction of the thumb occurs mainly at the CMC joint; thus, the adduction/abduction freedom at the MCP joint of the thumb can be ignored [15]. The proximal and distal joints have only one degree of freedom for bending and stretching, which are achieved through independent or coupled movements of each joint. According to the reference [16], the average value of the range of motion of each joint of the human finger is shown in Table 1, which is the average value of the angle of motion of the joints in normal adults.

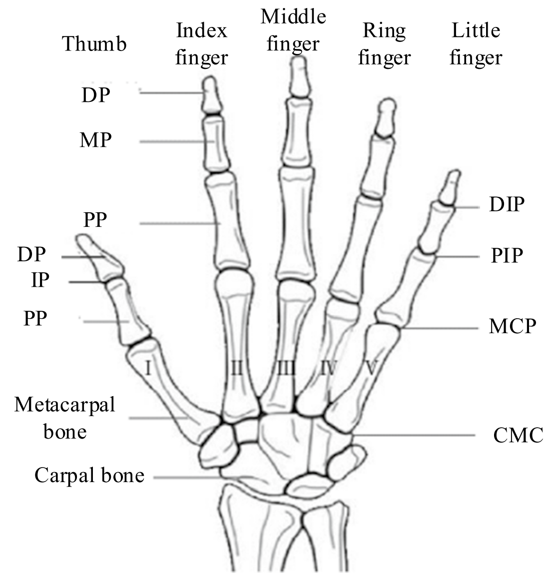

Fig. 1 Schematic diagram of the human hand skeleton

In the design of the rehabilitation hand, the range of motion of the finger joints of the human hand needs to be fully considered. From the perspective of rehabilitation training, it is necessary that the rehabilitation mechanism can provide as large a range of motion as possible, but not more than the range of motion of the finger joints shown in Table 1; otherwise, it may cause damage to the patient's hand [17]. Since the range of motion of the abduction/adduction degrees of freedom of the metacarpophalangeal joints of the four fingers in the daily grasping behavior of the human hand is small according to Table 1, this degree of freedom can be ignored during the training period, considering the modular design of the mechanical structure and the treatment needs

Table 1 The range of motion of the human hand joints

Finger area	Finger joints	Degree of freedom	Mode of motion	Range of motion (°)
Thumb	IP	1	Bend and stretch	0–80
	MCP	1	Bend and stretch	0–70
	CMC	2	Bend and stretch	0–70
			Adduction/abduction	0–20
the remaining four	DIP	1	Bend and stretch	0–80
	PIP	1	Bend and stretch	0 to 110
	MCP	2	Bend and stretch	− 20 to 80
			Adduction/abduction	− 20 to 20

Table 2 Finger joint diameters and corresponding finger knuckle lengths for adults in China (mm)

	MCP	PP	PIP	MP	DIP	DP
Thumb	26–29	45–55	16–18	20–35	14–17	28–33
Index finger	23–26	43–50	15–17	24–30	12–15	23–26
Middle finger	24–27	44–51	16–18	25–31	13–16	24–27
Ring finger	23–26	43–50	15–17	24–30	12–15	23–26
Little thumb	21–23	27–42	12–15	23–26	10–11	21–24

of patients with hand motor deficits in clinical medicine [18].

In addition to the need to consider the range of motion of the joints of the human hand, so that patients can achieve a large range of motion of the finger joints during rehabilitation training, it is also necessary to consider the knuckle length of the fingers so that the device can be applied to different sizes of hands as much as possible. Therefore, it is necessary to obtain a set of reference data that can reflect the range of human knuckle length. According to reference [19], the diameters of adult finger joints and the corresponding knuckle lengths are shown in Table 2.

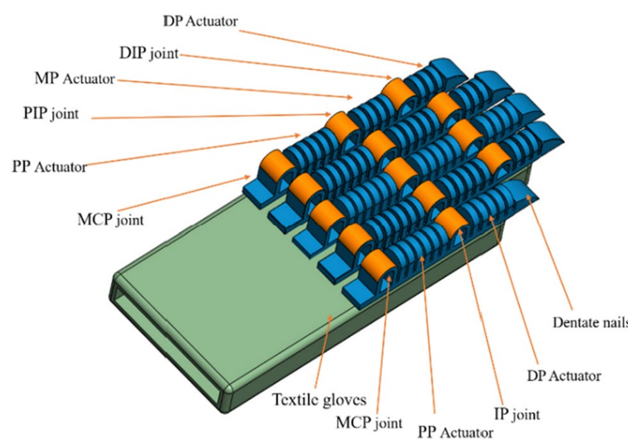

Fig. 2 Overall diagram of rehabilitation gloves

3 Overall structural design and deformation mechanism of rehabilitation hand

The pneumatically actuated segmented soft rehabilitation hand was designed based on the biological structure and motion characteristics of the human hand as shown in Fig. 2. The hand consists of various types of phalangeal actuators and cartilaginous joints, which are fixed to a soft knitted glove. Each segment of the phalangeal actuator can be flexed and extended with one degree of freedom under pneumatic actuation. With the linkage of the cartilage joint, the thumb rehabilitation finger is driven by two degrees of freedom through MCP actuator and DIP actuator, and the other four fingers are driven by three degrees of freedom through MCP actuator, PIP actuator, and DIP actuator. The total degree of freedom of the rehabilitation glove reaches 14, which can complete the reproduction of diversified gestures for people with impaired hand function.

3.1 Design of the actuator

The soft actuator adopts the form of a multi-chamber pneumatic grid structure and pneumatic drive mode. According to the bionic principle and finger structure, the height of the actuator decreases in order, and the top is semi-circular, the soft actuator consists of an air cavity, air pathway, and stoma, the actuator structure is shown in Fig. 3. The gas is fed into the air pathway through the stoma, so that the internal chamber of the actuator structure expands under the

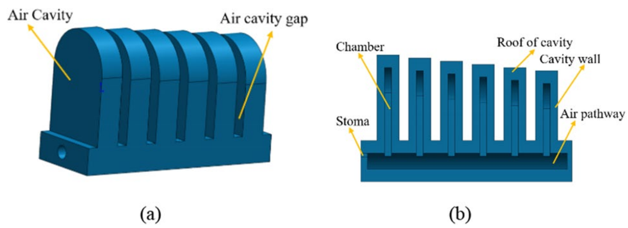

Fig. 3 The schematic of the actuator structure

Table 3 The structural dimension parameter of the actuator

Parameter	Numerical value/mm
Width of chamber	1.25
Cavity wall thickness	1.25
Air cavity gap	1.5
Cavity top thickness	2
Radius of the top circle of the chamber	6
Stoma radius	0.5
Width of air pathway	8

action of air pressure and generates a torque to achieve the bending effect and realize the driving effect of the actuator.

According to the human hand bionic principle, the fingers from the fingertip to the palm end from fine to coarse, through measuring a large number of different people's finger thickness data and analysis and summary, the design of adjacent air cavity height difference of 0.5 mm. The length of the driver is determined by the number of air cavities of the driver to a certain extent; the structure of the driver size parameters are shown in Table 3.

3.2 Single finger design

Due to the varying lengths and bending angles of the fingers, different numbers of air chambers are used in the design of each part of the rehabilitation finger actuator. The thumb is composed of a six-chamber actuator and a five-chamber actuator. The little finger is composed of a five-chamber actuator, a four-chamber actuator and a three-chamber actuator. The index finger and ring finger are formed by a combination of a six-chamber actuator, a five-chamber actuator, and a three-chamber actuator. The middle finger is a combination of a six-chamber actuator, a five-chamber actuator, and a four-chamber actuator. Different actuators on each finger are connected by soft joints. The shape of the soft joint is arch-shaped, and the material is high-density silicone, which plays a role in supporting and fixing the single finger, and at the same time has certain toughness and deformation when the single finger is bent and can fit the finger joint bending

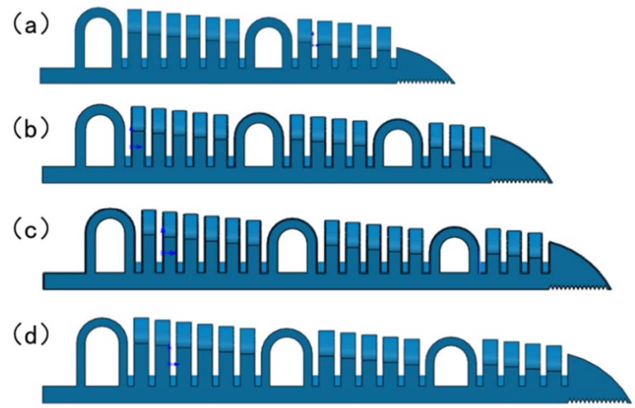

Fig. 4 Diagram of the different single fingers of the rehabilitated hand: **a** thumb rehabilitation finger, **b** little finger rehabilitation finger, **c** rehabilitation finger of index and ring finger, and d rehabilitation finger of middle finger

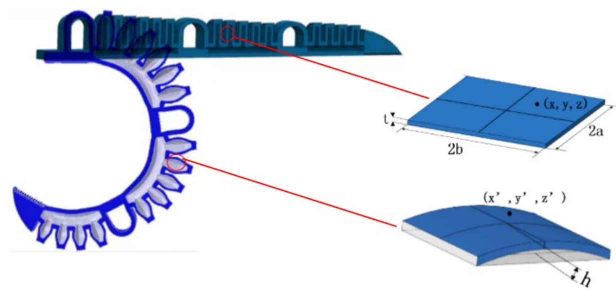

Fig. 5 Schematic diagram of the deformation of the sidewall of the air chamber of the actuator

for a certain degree of extension. The end of the rehabilitation single finger is designed as a dentate nail, which helps to increase friction when gripping things and is less likely to slip. The design of the rehabilitation finger structure adopts the parallel assembly of multiple drivers, so that a single driver drives a single bone joint of the finger and finally realizes the independent driving effect on each part of the finger. The single finger structure is shown in Fig. 4.

3.3 Rehabilitation of finger deformation mechanism

The lateral wall is simplified as an inflated elastomer rectangular membrane with the size of $2a \times 2b \times t$ and four edges clamped, as shown in Fig. 5. Its deformed profile is assumed to be a surface expressed by $z = hf(x/a)f(y/b)$, where h is the bulge height and $f(\tau)$ is called the profile function. Based on that, the displacement field u is provided by Eq. (1). Then, the total strain energy E is calculated through Eqs. (2) and (3), according to the second-order Yeoh's theory of hyperelasticity

$$u = \left[0,\ 0,\ hf(x/a)f(y/b)\right]^T \tag{1}$$

$$I_1 = tr\left[\left(I + \frac{\partial u}{\partial x}\right)\left(I + \frac{\partial u}{\partial x}\right)^T\right] \tag{2}$$

$$E = \int_{-t/2}^{t/2}\int_{-b}^{b}\int_{-a}^{a} C_1(I_1 - 3) + C_2(I_1 - 3)^2 \mathrm{d}x\mathrm{d}y\mathrm{d}z \tag{3}$$

where $x = (x, y, z)^T$ is the coordinate. I is the identity matrix of 3×3. I_1 is the first strain invariant. C_1 and C_2 are coefficients determined by the hyperelastic material properties.

Based on Eq. (3), total strain energy E of the inflated membrane is finally expressed by Eq. (4), which is directly related to the bulge height h

$$\begin{aligned} E = {} & 4C_2[A_0A_1(r^2 + 1/r^2) + 2C^2]h^4t/s \\ & + 4C_1B_0B_1(r + 1/r)h^2t \end{aligned} \tag{4}$$

where

$$A_0 = \int_0^1 [f(\tau)]^4 \mathrm{d}\tau, A_1 = \int_0^1 [f'(\tau)]^4 \mathrm{d}\tau,$$

$$B_0 = \int_0^1 [f(\tau)]^2 \mathrm{d}\tau, B_1 = \int_0^1 [f'(\tau)]^2 \mathrm{d}\tau,$$

$$C = \int_0^1 [f(\tau)]^2[f'(\tau)]^2 \mathrm{d}\tau \tag{5}$$

are constant only determined by the profile function $f(\tau)$. s $= ab$ and $r = b/a$ are the quarter area and aspect ratio of the membrane, respectively. To associate the inflating pressure P with the bulge height h, the principle of virtual work is used, i.e., Eq. (6). The left-hand side is virtual change of the total strain energy concerning to the bulge height and the right-hand side is virtual work done by the inflating pressure

$$[\mathrm{d}E(h)/\mathrm{d}h]\delta h = P[\mathrm{d}V(h)/\mathrm{d}h]\delta h \tag{6}$$

$$P = [4C_2/D^2]\,[A_0A_1(r^2 + 1/r^2) + 2C^2]\,h^3t/s^2 + kh \tag{7}$$

where $k = [2C_1B_0B_1/D^2]\,(r + 1/r)\,t/s$ and

$$P = [4C_2/D^2]\,[A_0A_1(r^2 + 1/r^2) + 2C^2]\,h^3t/s^2 \tag{8}$$

To determine the constants A_0, A_1, C, and D in Eq. (8) according to Eq. (5), we need to select an appropriate profile function $f(\tau)$. Generally, $f(\tau)$ should comply with actual deformation of the membrane as follows:

1. $f(\tau)$ is defined and monotonically decreases in the range $\tau \in [0, 1]$;
2. Maximum deformation occurs at center: $f(0)=1$;
3. Clamped edges are stationary: $f(1)=0$;
4. Membrane is smooth at center: $f'(0)=0$.

To simplify the calculation, a parabolic profile function $f(\tau) = 1 - \tau^2$ is selected. Then, the constants are calculated according to $f(\tau)$, which results in $A_0 = 0.406$, $A_1 = 3.2$, $C = 0.305$, $D = 0.667$. The material coefficients C_1 and C_2 for the elastomer have been determined by tension testing with rubber testing machines according to the standard ASTMD412 and then curve fitting, which results in $C_1=0.125$ and $C_2=0.0075$. Finally, by substituting these constants into equation Eq. (8), the relationship between the pressure inside the chamber and the deformation height can be found.

4 Rehabilitation finger simulation analysis and experimental validation

4.1 Rehabilitation finger movement simulation analysis

The motion simulation analysis of the rehabilitation finger can effectively check the structural rationality. The finite element simulation of the fluid cavity domain of the hyperelastic model of the three-dimensional model of the finger is carried out by ABAQUS software to analyze the force and deformation of different fingers. By changing the internal pressure of each drive cavity of the rehabilitation finger, the effect of motion deformation of the model under different pressure conditions is realized. The specific simulation process is as follows. First, the finger 3D model is imported, then the material properties of the assembly parts are defined, then the loads and boundary conditions are set, followed by the analysis step and force field output, then the fluid properties and interaction relations are input, then the meshing is performed, then the model is solved, and finally, the post-processing and the results are reported.

According to the design requirements of the rehabilitation finger, the Yeoh model is selected to define the material properties of the actuator, and the binding constraint is set between the actuator and the soft joint, the contact surface of the actuator is set as the slave surface, the soft joint connection surface is set as the master surface, and the rest of each actuator cavity wall adopts the self contact interaction type. The cavity point and fluid cavity are set in the actuator's cavity body, and the bending deformation of the rehabilitation finger model is solved using the input of different pressure values. The boundary condition of the metacarpal end is set to full constraint. The mesh is divided into a hexahedral structure with a global seed layout size of 1.2. The internal cavity of the actuator's has a complex structure, so the mesh is divided into a tetrahedral structure with a global seed layout size of 0.6, which ensures that the slave surface mesh is finer than the main surface mesh. The job is submitted for solving. The actuators material parameters are shown in Table 4.

4.2 Production of rehabilitation fingers

In the process of rehabilitation finger fabrication, the soft actuators and soft joints were fabricated separately by casting method. Because the number of air cavities in different parts of the actuator differs, each actuator mold is not designed with the exact same structure. The molds were designed separately according to the structure of the soft joints. All molds were molded by a 3D printing process using a resin material. During the casting and molding process, a thermostat was used at a temperature of 62 °C for about 4 h in order to accelerate the solidification of the silicone into the mold. Silicone glue was used to bond the contact surface between the casted actuator and the flexible joint, and the rest of the four fingers of the rehabilitation finger prototype were assembled in the same way as above (Fig. 6).

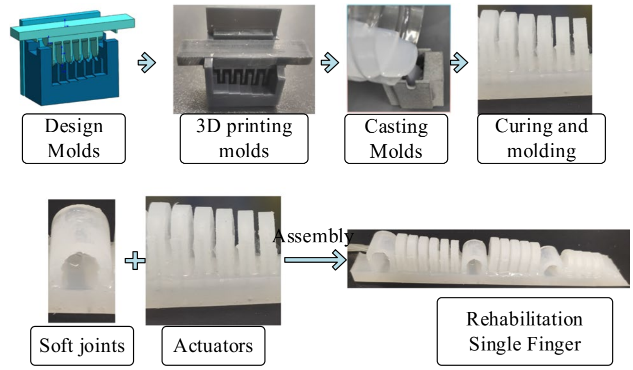

Fig. 6 The process of making rehabilitation fingers

4.3 Construction of an experimental platform for rehabilitation finger movements

After completing the finite element simulation for rehabilitating fingers, a single finger motion experiment platform was established to verify the correctness of the simulation, as shown in Fig. 7. Taking the index finger as an example, a high-speed camera system was used to measure the bending angle of the rehabilitated single finger under different pressures, test the characteristics of the soft actuator, and experimentally analyze the three-joint motion process of the rehabilitated finger. In the construction of the rehab finger bending experiment platform, the lens was installed on the camera; then, the camera was fixed on a tripod, and the high-speed camera circuit was connected. By adjusting the tripod to keep the camera lens in a good position with the rehab finger, the rehab finger was positioned in the center of the image.

During the measurement process, high-pressure gas was output through the air pump and regulated to the specified pressure by a precision pressure reducing valve. From 10 to 60 kPa, the pressure was successively output to the rehab finger. After the rehab finger was stably bent and deformed under the specified pressure, the high-speed camera was used to record the bending trajectory of the rehab finger. The angle measurement function on the display screen was used to read and record the bending angle value of the rehab finger at that pressure.

To verify whether the driving force generated by a finger-like actuator meets the requirements of human finger movements, it is necessary to test the output force of the actuator. The experimental platform consists of a computer, a pressure sensor, a finger-like actuator, a fixed seat, and a signal amplifier. In the process of measuring the output force of the actuator, the pressure sensor and the soft actuator are installed inside the fixed seat, and the bottom of the soft actuator is brought into close contact with the pressure sensor. When pressure is applied to the soft actuator, a driving force is generated at the end of the soft actuator, which acts on the pressure sensor. At this time, the sensor converts the force into a corresponding electrical signal, which is amplified by the signal amplifier and transmitted to the computer through a connecting line. The computer reads and processes the collected pressure data through specific software. During the measurement, the output force data of the actuator under different pressures are obtained by adjusting the pressure relief valve to obtain different driving force data generated by the soft actuator under different pressures, which are then analyzed (Fig. 8).

Table 4 Material parameters of the actuator

Hyperelastic material model coefficients	C_1	C_2	D_1
Numerical value	0.125	0.0075	0

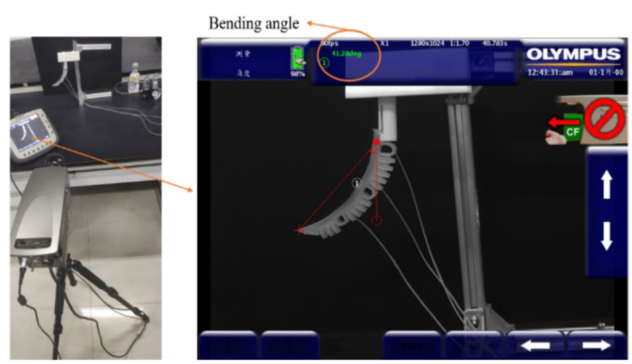

Fig. 7 The experimental platform for rehabilitating finger movements

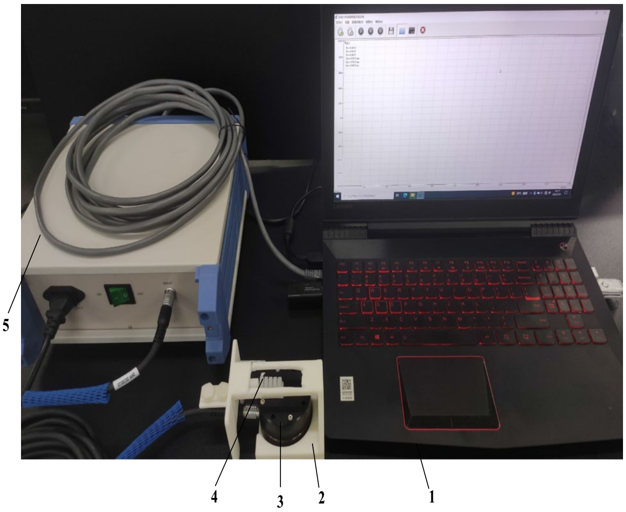

Fig. 8 The test platform for actuator drive: 1. computer, 2. fixed seat, 3. pressure sensor, 4. finger-like actuator, and 5. signal amplifier

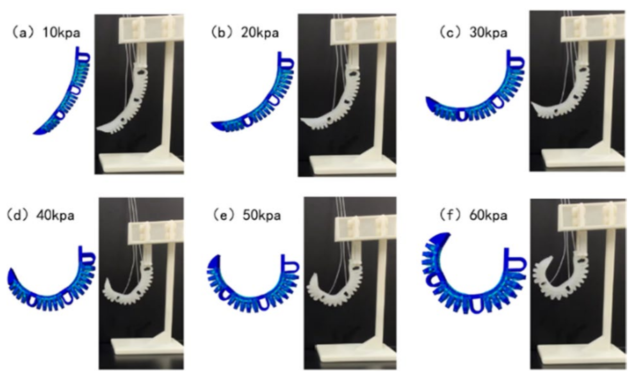

Fig. 9 Bending angle comparison between simulation and prototype experiments at typical air pressure values

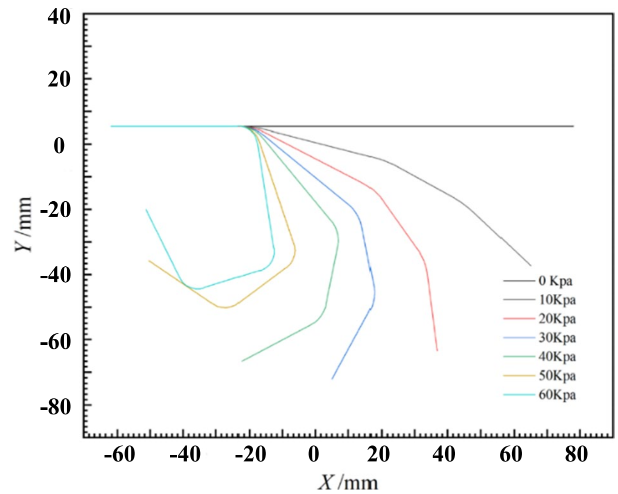

Fig. 10 The motion trajectory of a single finger

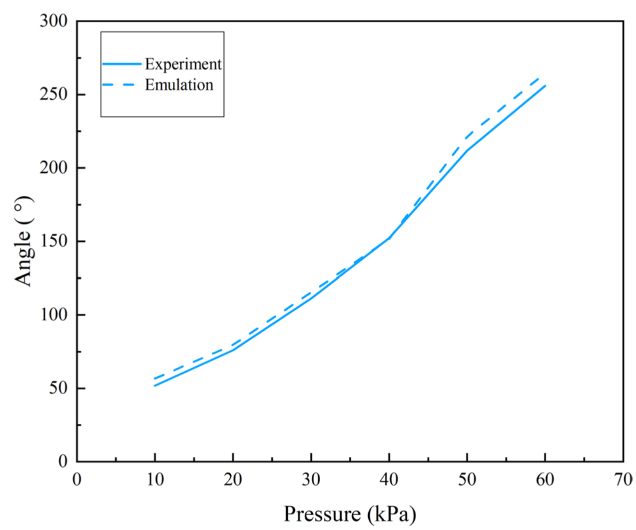

Fig. 11 Comparison of single finger bending angle between motion simulation and prototype experiment

4.4 Simulation and experimental comparison of rehabilitative finger movements

Comparing the experimental results of the rehabilitation finger motion with the simulation results, as shown in Fig. 9, it can be seen that the three joints are inflated simultaneously and there is a head-to-tail connection of the soft actuator. The motion trajectory of the rehabilitation single finger driving three joints simultaneously from 0 to 60 kPa and the bending angle was recorded, and the results are shown in Figs. 10 and 11. The simulation results can better simulate the experimental motion process and conform to the motion characteristics of the human hand when clenching a fist, which can realize the hand motion rehabilitation as well as the auxiliary motion function. The fingertip position gradually bends near the metacarpal joint as the air pressure increases, forming a similar polygonal fist shape. The bending angle of the single finger increases with the increase of air pressure and is limited by the elasticity of the silicone rubber material itself, the bending rate increases first and then decreases during the process of increasing pressure, and the bending angle recorded in the experimental data is slightly smaller than the bending angle of the simulation results, because the simulation is in an ideal state, ignoring the gravity of the rehabilitation single finger itself and other external factors. Finally, as shown in Table 5, a comparison of the analysis of bending angles with similar literature reveals that the bending angles of the rehabilitation finger designed by us can achieve satisfactory results.

By analyzing the driving force experimental data, the results are shown in Fig. 12. In the output pressure detection experiment of the rehabilitation glove actuator, the drive

Table 5 Similar literature on analysis of bending angles

	Fabrication	Pressure (kPa)	Angle
Our design	Silicone	60	250°
Ref. [20]	Silicone rubber	60	200°
Ref. [21]	Silicone	60	40°
Ref. [22]	Hyperelastic silicone + Fiber	60	90°
Ref. [23]	RTV silicone	60	30°

pressure shows a certain linear trend with the increase of air pressure, and the more air cavities there are at the same pressure, the greater the drive force. When the pressure is small, the difference in driving force produced by different air cavities of the actuator is smaller. In the experimental process, the actuator with a number of air chambers of 3 will swell when the pressure exceeds 100 kPa, and the maximum bearing pressure is 100 kPa.

4.5 Rehabilitation hand-assisted grasping experiment

The gripping action of fingers plays a pivotal role in facilitating fundamental activities in daily life, such as writing, drinking, eating, and object manipulation. To assess the rehabilitative hand's performance in grasping capabilities, experimental tests were conducted using representative objects, as illustrated in Fig. 13. The rehabilitative hand adeptly engages in a five-finger grasp to seize larger objects, maintaining a relaxed state in both fingers and muscles. Propulsive force transmitted through the dorsal side of the fingers during pressurization provides output force. Through

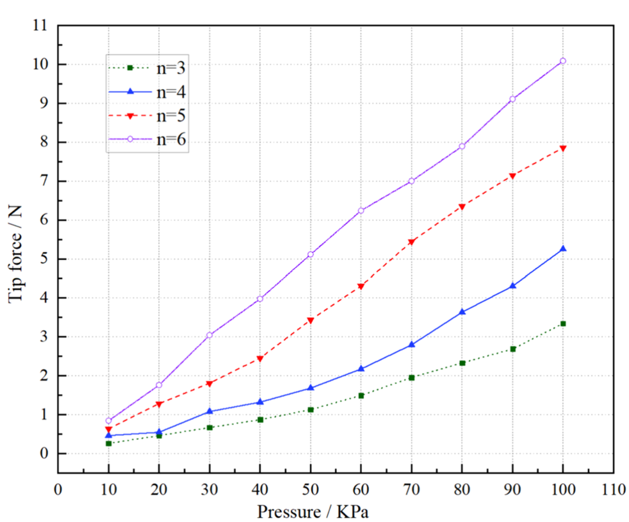

Fig. 12 The relationship between pressure and driving force of different number of cavity actuators

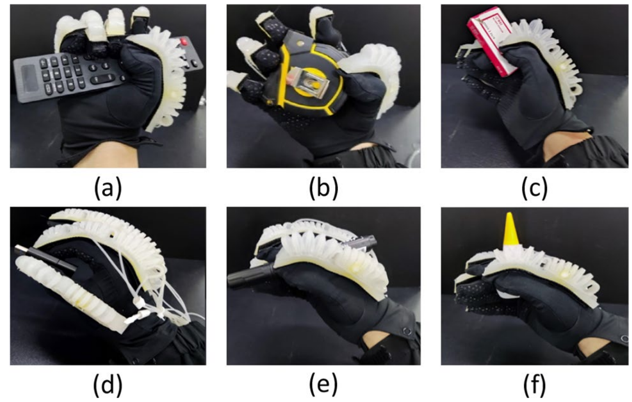

Fig. 13 The items grasped after wearing the rehabilitative hand: **a** and **b** represent schematic diagrams of holding the object and **c**–**f** represent schematic diagrams of grasping the object

assisted gripping, the rehabilitative hand demonstrates stable manipulation of objects with varying weights, including irregularly shaped items such as remote controls and tape measures. For smaller and lighter items like USB drives, glue, staples, and pens, the rehabilitative hand employs a flexible range of motions, achieving two-finger pinch, three-finger grasp, and five-finger envelopment. This versatile approach meets the demands of intricate actions in daily life.

5 Conclusion

In this paper, a pneumatically driven segmented multi-degree-of-freedom soft rehabilitation glove is designed and produced to help patients with hand dysfunction to perform finger rehabilitation exercises. The overall mechanism is designed to be lightweight, and the inherent softness of the soft material makes the whole mechanism more comfortable and convenient to wear. The entire structure of the rehabilitation glove can also drive the single joint of the finger while achieving the driving effect of the finger, which is more conducive to the realization of subtle finger manipulation. The following conclusions were reached during the study of the soft rehabilitation glove.

(1) The individual finger assembly relationship is expressed, the size of each joint skeleton of the rehabilitation finger is determined, and the feasibility of the structure is verified by finger prototype experiments.
(2) Based on the deformation analysis of the rehabilitation hand, finite element simulation analysis of the rehabilitation finger motion was performed and compared with the experimental results of finger bending. The comparison results showed that the trajectory of the single finger bending motion was in accordance with the motion characteristics of the human hand, and

the error between the experimental data and simulation results of the bending angle was small. The driving force experiment can understand the relationship between the pressure of different air cavity actuators and the driving force, which shows the potential of this soft body actuator in hand rehabilitation.

Author contributions Huadong Zheng and Wei Bai conceived and designed the study. Wei Bai and Linxiao Liu performed the experiments. Caidong Wang wrote the paper. Huadong Zheng, Caidong Wang, and Xinjie Wang reviewed and edited the manuscript. All authors read and approved the manuscript.

Funding This work was supported by Scientific and technological breakthroughs in Henan Province (No. 222102220101), and (No. 232102221031).

Declarations

Conflict of interest The authors declare no competing interests.

Ethical approval This manuscript does not contain any studies with human participants or animals.

Consent to participate All the authors provided their consent.

Consent for publication All the authors have read and agreed to publish this manuscript.

References

1. Sut DJ, Sethuramalingam P (2023) Soft manipulator for soft robotic applications: a review. J Intell Robot Syst 108:10. https://doi.org/10.1007/s10846-023-01877-4
2. Shen Z, Chen F, Zhu X, et al (2020) Stimuli-responsive functional materials for soft robotics. J Mater Chem. B(39)
3. Rehman T, Faudzi AAM, Dewi DEO et al (2017) Design, characterization, and manufacturing of circular bellows pneumatic soft actuator. Int J Adv Manuf Technol 93:4295–4304. https://doi.org/10.1007/s00170-017-0891-z
4. Janghorban A, Dehghani R (2022) Design and motion analysis of a bio-inspired soft robotic finger based on multi-sectional soft reinforced actuator. J Intell Robot Syst 104:74. https://doi.org/10.1007/s10846-022-01579-3
5. Feng N, Shi Q, Wang H et al (2018) A soft robotic hand: design, analysis, sEMG control, and experiment. Int J Adv Manuf Technol 97:319–333
6. Carneiro J, Almeida F, Pinto J (2019) Endurance tests of a linear peristaltic actuator. Int J Adv Manuf Technol 100:2103–2114. https://doi.org/10.1007/s00170-018-2858-0
7. Fan J, Wang S, Yu Q, Zhu Y (2020) Swimming performance of the frog-inspired soft robot. Soft Robot 7:615–626. https://doi.org/10.1089/soro.2019.0094
8. Yurkewich A, Kozak IJ, Hebert D et al (2020) Hand extension robot orthosis (hero) grip glove: enabling independence amongst persons with severe hand impairments after stroke. J NeuroEng Rehabilit 17:33. https://doi.org/10.1186/s12984-020-00659-5
9. Chen J (2019) Research on a soft-software actuator—driven hand rehabilitation exoskeleton. Southeast University
10. Takahashi N, Furuya S, Koike H (2020) Soft exoskeleton glove with human anatomical architecture: production of dexterous finger movements and skillful piano performance. IEEE Trans Haptics 13(4):679–690. https://doi.org/10.1109/TOH.2020.2993445
11. Polygerinos P, Correll N, Morin SA et al (2017) Soft robotics: review of fluid-driven intrinsically soft devices; manufacturing, sensing, control, and applications in human-robot interaction. Adv Eng Mater 19:1700016. https://doi.org/10.1002/adem.201700016
12. Wang LZ, Peng GS, Yao W et al (2020) Intelligent biomechatronics in neurorehabilitation soft robotics for hand rehabilitation. Pp 167–176. https://doi.org/10.1016/B978-0-12-814942-3.00010-6
13. Alibadi A, Neftimeziani S, Davis S (2020) The design, kinematics and torque analysis of the self-bending soft contraction actuator. Actuators 9(2):33. https://doi.org/10.3390/act9020033
14. Serbest K, Cilli, Yildiz MZ, Eldogan O (2016) Development of a human hand model for estimating joint torque using MATLAB tools. In: 2016 6th IEEE international conference on biomedical robotics and biomechatronics (BioRob), Singapore, pp 793–797. https://doi.org/10.1109/BIOROB.2016.7523724
15. Cappello L, Galloway KC, Sanan S et al (2018) Exploiting textile mechanical anisotropy for fabric-based pneumatic actuators. Soft Rob 5(5):662–674
16. Bi Q (2015) Research on the basic theory of hand exoskeleton system and its control technology. Zhejiang University
17. Leonardo C, Jan T, Meyer, Kevin C et al (2018) Assisting hand function after spinal cord injury with a fabric-based soft robotic glove. J NeuroEng Rehabilit (1)
18. Garriga-Casanovas A, Collison I et al (2018) Toward a common framework for the design of soft robotic manipulators with fluidic actuation. Soft Robot 5(5):622–649. https://doi.org/10.1089/soro.2017.0105
19. GB/T 16252-1996, Hand sizing system—adult. Beijing, China Standards Press (1996)
20. Sun Z, Guo Z, Tang W (2019) Design of wearable hand rehabilitation glove with soft hoop-reinforced pneumatic actuator. J Cent South Univ 26(1):106–119. https://doi.org/10.1007/s11771-019-3986-x
21. Rehman T, Faudzi A, Octorina D et al (2016) Design and analysis of bending motion in single and dual chamber bellows structured soft actuators. J Teknol. https://doi.org/10.11113/jt.v78.9267
22. Wang Z, Polygerinos P, Overvelde J et al (2017) Interaction forces of soft fiber reinforced bending actuators. IEEE/ASME Trans Mechatron 22(2):717–727. https://doi.org/10.1109/TMECH.2016.2638468
23. Udupa G, Sreedharan P, Sai D et al (2014) Asymmetric bellow flexible pneumatic actuator for miniature robotic soft gripper. J Robot 1:1–11. https://doi.org/10.1155/2014/902625